Journal of Experimental Botany, Vol. 59, No. 12, pp. 3485–3499, 2008
doi:10.1093/jxb/ern201 Advance Access publication 06 August, 2008
This paper is available online free of all access charges (see http://jxb.oxfordjournals.org/open_access.html for further details)

Journal of Experimental Botany
www.jxb.oxfordjournals.org

RESEARCH PAPER

Arabidopsis sterol carrier protein-2 is required for normal development of seeds and seedlings

Bing Song Zheng[1,2], Elin Rönnberg[1], Lenita Viitanen[3], Tiina A. Salminen[3], Krister Lundgren[4], Thomas Moritz[4] and Johan Edqvist[5,*]

[1] *Department of Plant Biology and Forest Genetics, Swedish University of Agricultural Sciences, PO Box 7080, 750 07 Uppsala, Sweden*

[2] *School of Forestry and Biotechnology, Zhejiang Forestry University, 311300, Lin An, China*

[3] *Department of Biochemistry and Pharmacy, Åbo Akademi University, Artillerigatan 6 A III, FIN-20520 Turku, Finland*

[4] *Umeå Plant Science Center, Department of Forest Genetics and Plant Physiology, Swedish University of Agricultural Sciences, 901 83 Umeå, Sweden*

[5] *IFM Biology, Linköping University, 581 83 Linköping, Sweden*

Received 25 April 2008; Revised 27 June 2008; Accepted 4 July 2008

Abstract

The *Arabidopsis thaliana* sterol carrier protein-2 (AtSCP2) is a small, basic and peroxisomal protein that *in vitro* enhances the transfer of lipids between membranes. AtSCP2 and all other plant SCP-2 that have been identified are single-domain polypeptides, whereas in many other eukaryotes SCP-2 domains are expressed in the terminus of multidomain polypeptides. The AtSCP2 transcript is expressed in all analysed tissues and developmental stages, with the highest levels in floral tissues and in maturing seeds. The expression of AtSCP2 is highly correlated with the multifunctional protein-2 (MFP2) involved in β-oxidation. *A. thaliana Atscp2-1* plants deficient in AtSCP2 show altered seed morphology, a delayed germination, and are dependent on an exogenous carbon source to avoid a delayed seedling establishment. Metabolomic investigations revealed 110 variables (putative metabolites) that differed in relative concentration between *Atscp2-1* and normal *A. thaliana* wild-type seedlings. Microarray analysis revealed that many genes whose expression is altered in mutants with a deficiency in the glyoxylate pathway, also have a changed expression level in *Atscp2-1*.

Key words: Arabidopsis, β-oxidation, germination, glyoxylate cycle, lipid, lipid transport, metabolomics, microarray, peroxisomes, SCP-2.

Introduction

Sterol carrier protein-2 (SCP-2) is an intracellular, small, basic protein domain that *in vitro* stimulates the transfer of lipids between membranes (Ritter *et al*., 1971; Bloj *et al*., 1978). In mammals, SCP-2 is implicated to have role in peroxisomal β-oxidation. The exact function of SCP-2 in β-oxidation is unclear, but it might facilitate the presentation and solubilization of the substrates or stabilizing the enzymes involved in catalysing the reaction cycles (Seedorf *et al*., 2000). Such suggestions are mainly based on studies of the mammalian peroxisomal proteins sterol carrier protein-X (SCP-X) and D-bifunctional protein (DBP), which both contain C-terminal SCP-2 domains. The human gene *SCPX* (also known as *SCP2*) encodes SCP-X, which consists of a 3-ketoacyl-CoA thiolase domain connected to a C-terminal SCP-2 domain (Ohba *et al*., 1994). Due to the existence of dual promoters, as well as proteolytic cleavage sites the *SCPX* encoded SCP-2 domain is also expressed as a single-domain protein (Ohba *et al*., 1995). SCP-X and the single-domain SCP-2 are both predominantly located to peroxisomes. Gene

* To whom correspondence should be addressed: johed@ifm.liu.se

targeting in mice revealed that complete deficiency of *SCPX* resulted in an impaired catabolism of 2-methyl branched-chain fatty acyl CoAs as shown by a 10-fold accumulation of phytanic acid in *SCPX*(–/–) mice (Seedorf *et al*., 1998). Further, it has been demonstrated with FRET microscopy that the single-domain SCP-2 interacts in peroxisomes with enzymes involved in β-oxidation such as acyl-CoA oxidase, bifunctional protein, and 3-ketoacyl-CoA thiolase (Wouters *et al*., 1998). It may be noteworthy that plants are not encoding any gene orthologous to the 3-ketoacyl-CoA thiolase in SCP-X (Edqvist and Blomqvist, 2006).

A SCP-2 domain is also present in the C-terminus of the mammalian DBP (also referred to as MFE-2), which in the human genome is encoded from *HSD17B4*. DBP has domains for D-3 (equivalent to *3R*)-hydroxyacyl-CoA dehydrogenase, 2-enoyl-CoA hydratase, and SCP-2 (Adamski *et al*., 1995; Leenders *et al*., 1998) and catalyses the second and third steps of the β-oxidation pathway. Reactions catalysed by the mammalian DBP proceed through D-3-hydroxyl-CoA esters. DBP is suggested to be required for the peroxisomal β-oxidation of the enoyl-CoA esters of very long chain fatty acids, pristanic acid, and of dihydroxycholestanoic acid (DHCA) (Wanders, 2004). The role of the SCP-2 domain in DBP is unclear, but it contains a peroxisomal targeting signal (PTS1) that locates DBP to the peroxisomes. The structural and functional conservation may indicate that the SCP-2 domain in DBP also has additional functions, such as to interact with enzymatic domains of DBP to form an extended hydrophobic cavity for the hydrophobic tails of some β-oxidation substrates (Haapalainen *et al*., 2001).

A. thaliana do not encode DBP, and there are no plant genes identified orthologous to the D-3-hydroxyacyl-CoA dehydrogenase domain of mammalian DBP (Edqvist and Blomqvist, 2006). Rather, the *A. thaliana* multifunctional proteins AIM1 and MFP2 each share domain structure and approximately 50% amino acid sequence similarity to the human peroxisomal L-bifunctional protein (LBP) (also referred to as MFE-1) (Kiema *et al*., 2002). LBP and DBP lack significant sequence similarity and LBP, as well as AIM1 and MFP2, are not carrying any C-terminal SCP-2 domain. Furthermore, reactions catalysed by LBP, AIM1, and MFP2 proceeds through L-3-hydroxyl-CoA esters.

Thus, plants do not encode DBP or SCP-X, but it has recently been shown that plants also encode and express SCP-2 (Eklund and Edqvist, 2003; Edqvist *et al*., 2004; Edqvist and Blomqvist, 2006). The gene *AtSCP2* (At5g42890) on chromosome 5 encodes the sole SCP-2 domain in the *A. thaliana* genome. AtSCP2 is a 13.6 kDa protein with a p*I* of 9.2, which localizes to peroxisomes through its C-terminal PST1 targeting signal. It has lipid transfer activity *in vitro* (Edqvist *et al*., 2004). The known crystal structures of SCP-2 from rabbit (Choinowski *et al*., 2000), of the SCP-2 domain of the human DBP (Haapalainen *et al*., 2001) and of yellow fever mosquito SCP-2 (Dyer *et al*., 2003) have an α/β-fold consisting of a five stranded β-sheet and four or five α-helices. A C-terminal segment, together with part of the β-sheet and four α-helices form a hydrophobic tunnel, which is very suitable for binding of lipids or other hydrophobic ligands. According to generated models, AtSCP2 has a similar α/β-fold forming a hydrophobic tunnel (Edqvist *et al*., 2004). AtSCP2 and also all other plant SCP-2 that have been identified are single-domain polypeptides (Edqvist and Blomqvist, 2006; Viitanen *et al*., 2006), whereas, as indicated above, SCP-2 domains in animals and many other eukaryotes are often present in the terminal of polypeptides which carry multiple protein domains.

The only SCP-2 domain encoded in *A. thaliana* is the single-domain protein AtSCP-2. As described above and in Edqvist and Blomqvist (2006), the situation is more complex in animals, with larger SCP-2 gene families and often quite complicated arrays of protein domain fusions. We reason that this turns *A. thaliana* into a very suitable model organism for studying the function of the still enigmatic SCP-2 domain. Here, an initial investigation on the biological function of AtSCP2 is presented. It is shown that the activity of the peroxisomal protein AtSCP2 is important for the metabolism in *A. thaliana* seeds and seedlings.

Materials and methods

Plant materials and growth conditions

A. thaliana ecotype Columbia (Col-0) was used as the wild-type plant. Seeds of the T-DNA insertion lines Sail_1231_F11 were purchased from the European Arabidopsis Stock Centre (NASC) (Loughborough, UK). The Sail_1231_F11 line is referred to as *Atscp2-1*. Seeds were surface-sterilized (washed in 70% ethanol for 1 min and in 15% chlorine and 0.5% SDS for 10 min followed by at least four washes in sterile distilled water) and sown on half-strength Murashige and Skoog medium (1/2 MS). Before cultivation, seed dormancy was broken by 72 h of cold treatment (4 °C). The synthetic auxin 2,4-dichlorophenoxybutyric acid (2,4-DB) (0.1 μM, 4 μM) and indole-3-butyric acid (IBA) (3 μM, 30 μM) were added to the autoclaved medium where indicated. Ten-day-old plants grown under sterile conditions were transplanted on soil mixed with vermiculite (2:1 v/v). The plants were cultivated under controlled conditions in environmental chambers at 20–22 °C under long day (16/8 h light/dark) conditions. The *Atscp2-1* mutant was back-crossed to wild-type *A. thaliana* Col-0.

For expression of AtSCP2 in *Atscp2-1* under the control of its own promoter, a DNA fragment carrying the *AtSCP2* gene including the promoter was obtained through amplification of *A. thaliana* genomic DNA with primers ATSCP2promattB1F (5′-GGGGACAAGTTTGTACAAAAAAGCAGGCTCACACCTCCT-ATTTATCGGACAT-3′) and AtSCP2attB2R (5′-GGGGACCACT-TTGTACAAGAAAGCTGGGTTCACAACTTTGAAGGTTTACG-GAAGAT-3′). The PCR fragment was recombined into the destination vector pMDC99 (Curtis and Grossniklaus, 2003) resulting in the plasmid pJE602. For expression of AtSCP2 cDNA under control of the cauliflower mosaic virus (CaMV) 35S promoter, a fragment carrying a cDNA copy of *AtSCP2* was

amplified from *A. thaliana* cDNA with ATSCP2attB1F (5′-GGGGACAAGTTTGTACAAAAAAGCAGGCTATGGCGAATA-CCCAACTCAAATC-3′) and ATSCP2attB2R. The PCR fragment was recombined into destination vector pMDC32 (Curtis and Grossniklaus, 2003) yielding plasmid pJE601. Recombination events were done with the Gateway technology from Invitrogen (Carlsbad, CA, USA). pJE601 and pJE602 were transformed into *Agrobacterium tumefaciens* C58. The floral dip method (Clough and Bent, 1998) was used to transform *A. thaliana Atscp2-1* with *A. tumefaciens* C58 carrying pJE601 or pJE602. Transformations and selection of transformants were done at the Uppsala Transgenic Arabidopsis Facility. The transformants obtained were denoted *Atscp2-1*(*35S*::*AtSCP2*) for transformation with pJE601 and *Atscp2-1*(*AtSCP2*::*AtSCP2*) for transformation with pJE602.

Phenotypic assays

The hypocotyl and root lengths were measured on 3-d-old and 7-d-old seedlings grown on ½ MS medium with 0% or 1% sucrose. At least 20 seedlings were measured from each growth condition and time point. All experiments were performed in triplicate. Rosette diameter was measured at the widest point of the plant without disturbing any leaves under light. The developing seeds were counted after self-pollination. The percentage of seed germination was scored every 12 h after transferring stratified seeds on the MS media to a growth chamber. Germination was defined as an obvious protrusion of the radicle through the seed coat. Several seed lots were tested with similar results.

Histochemical and quantitative GUS activity assays

A DNA fragment carrying the *AtSCP2* promoter was amplified from the *A. thaliana* Col-0 genome by the use of primers SCPPrU2 (5′-CACACCTCCTATTTATCGGACAT-3′) and SCPPrN2 (5′-GATTTTTGTTAGAGACTGGCACG-3′). The PCR primers were designed such that a fragment was amplified stretching from the untranslated region of the nearest gene upstream of *AtSCP2* to the 5’ untranslated region of *AtSCP2*. The obtained 1.4 kb *AtSCP2* promoter fragment was inserted into vector PCR2.1-TOPO (Invitrogen) to yield the plasmid pER2. The *AtSCP2* promoter fragment was released from pER2 by restriction enzymes *Xba*I+*Bam*H1, and subsequently fused to the β-glucuronidase (GUS) reporter gene by ligation to the *Xba*I+*Bam*H1 sites of vector pBI101 resulting in plasmid pER1. The plasmid pER1 was transformed to *A. tumefaciens* C58.

Histochemical GUS-assays were performed as described by Jefferson *et al*. (1987). Plant tissues were incubated in a substrate solution containing 50 mM Na-phosphate buffer (pH 7.0), 1 mM 5-bromo-4-chloro-3-indolyl-β-D-glucuronic acid cyclohexyl ammonium salt (X-GlcA CHA) (Duchefa Biochemie, Haarlem, The Netherlands), 0.5 mM $K_4Fe(CN)_6$, 0.5 mM $K_3Fe(CN)_6$, and 0.01% (w/v) Triton X-100 at 37 °C overnight. Stained samples were incubated in 95% ethanol at room temperature to extract the chlorophyll.

Quantitative real-time reverse transcriptase-PCR, reverse transcriptase-PCR and genomic PCR

RNA was extracted from *A. thaliana* using the Qiagen RNeasy Plant Mini Kit (Qiagen, Hilden, Germany). Five μg RNA was used for cDNA synthesis using oligo dT-primer and Superscript II Rnase-Reverse Transcriptase (Invitrogen) according to the manufacturer’s instructions. Amplification of the cDNA was performed in the presence of gene-specific primers and the SYBR Green PCR master mix (Applied Biosystems, Foster City, CA, USA) in MicroAmp Optical 96-well reaction plates with optical covers using an ABI Prism 7000 Sequence Detector (Applied Biosystems). Reaction conditions were 50 °C for 2 min, 94 °C for 10 min, followed by 40 cycles of 94 °C for 15 s and 60 °C for 1 min. All cDNA-samples were included in triplicate in all assays. Primers were designed using Primer express software (Applied Biosystems). Relative quantification of gene expression data was carried out with the $2^{-\Delta\Delta CT}$ or comparative C_T method (Livak and Schmittgen, 2001). The threshold cycle (C_T) indicates the cycle number at which the amount of amplified transcript reaches a fixed threshold. Expression levels were normalized with the C_T values obtained for the *A. thaliana* tubulin β-2/β-3 chain (At5g62690). The following gene-specific primers were used: AtSCP2: SCPF1 (5′-GCCGGGA-AAGAGGTCACA-3′) and SCPR1 (5′-TGTAAGTAACCTCTT-CAAACCCTAATTTCT-3); *A. thaliana* tubulin β-2/β-3 chain (At5g62690): Tub1 (5′-ACACCAGACATAGTAGCAGAAAT-CAAG-3′) and Tub2 (5′-GAGCCTTACAACGCTACTCTGTCT-GTC-3′); At3g21720: 3g21720F (5′-TTGCACAGATCGCAGAC-ATCA-3′) and 3g21720R (5′-GAATTGGGTGCATTCATTGA-GA-3′); At1g06570: 1g06570F (5′-CTCCGCCAAATCCGAT-CTT-3′) and 1g06570R (5′-GGAGGTCACCGGAGGTGAGT-3′); At3g47340: 3g47340F (5′-AACGTCTTGCCGTCATCGAT-3′) and 3g47340R (5′-CAATGGTCTTGTCCTCGTTGAA-3′); At1g08630: 1g08630F (5′-CGATGCGAGAAGCAATGTGTA-3′) and 1g08630R (5′-CGTCTAGCCGTTGGGTCATATC-3′); At1g21400: 1g21400F (5′-AGACACAGGCTGATCATTTGGTT-3′) and 1g21400R (5′-TTTGCCTCCTGGGAAATCC-3′); At3g45140: 3g45140F (5′-AGC-CCCAATGGAAACAAGTCT-3′) and 3g45140R (5′-AGCAAGAT-TCCATAGCCAGCA-3′); At5g55730: 5g55730F (5′-GGCACCAG-AGGATGGTGATG-3′) and 5g55730R (5′-TCTTTCCTTTCGCTT-TCCCTTT-3′); At5g04960: 5g04960F (5′-AAACGCGAGCCGAT-CAAG-3′) and 5g04960R (5′-AGAGCTCCGTGAT-GGTGACTTT-3′); At3g14210: 3g14210F (5′-CAGGAGGAAATGGCTCATCTTC-TA-3′) and 3g14210R (5′-AGCTCACGGACC-GTCATTG-3′); At1g52050: 1g52050F (5′-TTCCTAAGCTACAGAAGTTTGTTCA-TGCATG-3′) and 1g52050R (5′-CATAGTTGACAACATCGGAA-TCG-3′).

Reverse transcriptase-PCR (RT-PCR) was done as described previously (Edqvist *et al*., 2004). The oligonucleotides ATSCPRT1 and ATSCPRT2 were used for expression analysis of *AtSCP2* cDNA, while UBL1 and UBL2 were used for amplification of cDNA for the ubiquitin-conjugating enzyme E2-21 kD (At5g41340) (Edqvist *et al*., 2004).

For isolation of *A. thaliana* genomic DNA, 500 μl of an extraction buffer consisting of 200 mM TRIS, 250 mM NaCl, and 25 mM EDTA was added to plant tissues. After addition of six glass beads (3 mm in diameter), the tissues were disrupted by incubation in a FAST-prep instrument (MP Biomedicals, Irvine, CA, USA) for 30 s. 25 μl of 10% SDS was added, and the samples were incubated at 65 °C for 10 min and then centrifuged for 5 min. 450 μl of the supernatant was removed and precipitated with an equal volume of cold isopropanol. After incubation for 2 min at room temperature, samples were centrifuged for 5 min. The supernatant was discarded, and the DNA pellet obtained was dried, dissolved in water, and used for PCR. The following primers were used for analysing genomic DNA from *Atscp2-1*: SAIL_1231_F11_RP (5′-AACATTGCTCCAAAGGTTGGT-3′), SAIL_1231_F11_LP (5′-GGACCAAATCCAAGTCACACA-3′) and SAIL_LB1 (5′-GCCTTTTCAGAAATGGATAAATAGCCTTGC-3′).

Expression profiling through microarray analysis

Two-day-old seedlings of the *Atscp2-1* and wild-type plants grown under light conditions on 1/2 MS without sucrose were harvested and frozen quickly in liquid nitrogen. Two-day-old seedlings were selected for the expression analysis due to the high AtSCP-2 expression levels and the manifested phenotype of young *Atscp2-1*

seedlings when grown on 1/2 MS without exogenous carbon source. RNA samples were extracted using RNeasy Plant Mini Kit (Qiagen). Five μg of total RNA was converted to double-stranded cDNA using the SuperScript polymerase II (Invitrogen) with a T7-dT primer incorporating a T7 RNA polymerase promoter (Ambion, Austin, TX, USA). The double-stranded cDNA was amplified to cRNA through *in vitro* transcription using Megascript T7 kit (Ambion). To obtain aminoallyl-labelled cDNA the amplified cRNA was used as template for cDNA synthesis performed with SuperScript III (Invitrogen) in the presence of dATP, dCTP, dGTP, and aminoallyl-dUTP (aa-dUTP). After completion of cDNA synthesis unincorporated aa-dUTP was removed by using Qiagen QIAquick PCR purification kit. The purified aminoallyl-labelled cDNA (aa-cDNA) was lyophilized and subsequently dissolved in 4.5 μl of 0.1 M Na_2CO_3-buffer, pH 9.0. To label the aa-cDNA, 4.5 μl of the NHS-ester Cy3 or Cy5 dye, prepared in DMSO, was added and the mixture was incubated at room temperature for 1 h in darkness. The two resulting dye-labelled cDNA pools were mixed and then co-hybridized to the same *A. thaliana* CATMA microarray slide (Allemeersch *et al*., 2005) for 2 d at 42 °C in a water bath. After that, the arrays were washed and then scanned using a GenePix 4000B array scanner (Molecular Devices, Sunnyvale, CA, USA). The raw data were stored and analysed using BASE (https://base.lcb.uu.se) and the Linnaeus Centre for Bioinformatics (LCB) Data Warehouse (https://dw.lcb.uu.se) at LCB and the WCN Expression Array Facility at Uppsala University and The Swedish University of Agricultural Sciences, Uppsala, Sweden. Four replicates were made. The empirical Bayes methods B-statistics (Filtering Bstat1 >7.21) (Lönnstedt and Speed, 2002; Smyth *et al*., 2003; Lönnstedt and Britton, 2005) was applied to rank the genes in order of evidence for differential expression, from the strongest to the weakest evidence.

Metabolomics

Metabolites were extracted from 3-d-old seedlings of *A. thaliana* wild-type and *Atscp2-1*. Seedlings were grown on 1/2 MS without sucrose. The young seedlings were selected for metabolome profiling due to the high AtSCP-2 expression levels in wild-type and the manifested phenotype in young *Atscp2-1* seedlings when grown on 1/2 MS without sucrose. From each genotype, 10 samples of 20 mg fresh weight were used for the analysis. Extraction of metabolites, GC/MS analysis, and data processing were done as described previously (Gullberg *et al*., 2004; Jonsson *et al*., 2005). All multivariate statistical investigations (PCA, PLS-DA) were performed using Simca software 10.5.0.0 (Umetrics, Umeå, Sweden). The following statistics for the PLS-DA models are discussed throughout this paper: R^2X is the cumulative modelled variation in X, R^2Y is the cumulative modelled variation in Y and Q^2Y is the cumulative predicted variation in Y, according to cross-validation. The range of these parameters is 0–1, where 1 indicates a perfect fit.

Docking of auxin precursors into the homology model of Arabidopsis thaliana *SCP-2*

The docking program GOLD 3.2 (Jones *et al*., 1995, 1997) was used to dock the auxin precursors IBA and 2,4-DB into the previously created homology model of AtSCP-2 (Edqvist *et al*., 2004), which is based on the crystal structure of the SCP-2-like domain of human DBP (Haapalainen *et al*., 2001). The IBA and 2,4-DB structures were generated using the program SYBYL 8.0 (Tripos International, St Louis, MO, USA). Ten independent genetic algorithm runs with the default docking parameters were made in GOLD for the ligands. The binding site was restricted within a 15 Å radius of the side-chain hydrogen (HZ) of Phe112 in the AtSCP2 model. The docking was stopped if the three best scoring solutions were within 1.5 Å rmsd of each other. The cavity in the AtSCP2 model was identified using the program SURFNET (Laskowski, 1995). The docking results were visualized and examined in the BODIL modelling environment (Lehtonen *et al*., 2004).

Results

Expression of AtSCP2 *during development*

To gain insight on the expression pattern of *AtSCP2*, we analyzed large amount of data accessible in public databases (i.e. www.weigelworld.org, www.arabidopsis.org, and www.genevestigator.ethz.ch) from microarray analysis of gene expression during *A. thaliana* development. Figure 1 shows the expression of *AtSCP2* in 63 samples from different tissues or stages of development. The data are from the AtGenExpress expression atlas (www.weigelworld.org) (Schmid *et al*., 2005) and shows that the *AtSCP2* mRNA is present in all tissues and at all stages of the life of the plant. The highest levels of the *AtSCP2* transcript was found in seeds, such as in green cotyledons of maturating seeds (Fig. 1, sample 63), and in floral tissues, such as the stamens of stage 12 flowers (Fig. 1, sample 51) and petals (Fig. 1, sample 50) and stamens of stage 15 flowers (Fig. 1, sample 52). The accumulation of the *AtSCP2* transcript in roots, stems, buds, siliques, inflorescences, and leaves of mature *A. thaliana* plants was analysed with quantitative real-time RT-PCR (data not shown). The results obtained confirmed that the *AtSCP2* mRNA is abundant in most *A. thaliana* tissues.

The *A. thaliana AtSCP2* promoter was fused to the β-glucuronidase (GUS) reporter gene and the temporal and spatial patterns of expression were assessed during plant growth and development (Fig. 2). Endosperm (Fig. 2B), embryo (Fig. 2C), and 2-d-old seedlings (Fig. 2D) showed very high GUS activity. Staining was also detected in vascular tissues and hydathodes of cotyledons (Fig. 2E), in trichomes of the rosette leaves (Fig. 2F), in the receptacles (Fig. 2G, H), in vascular tissues of sepals and petals (Fig. 2G, I, J), in the style and stigma of the carpels (Fig. 2G, K), and in anthers, filaments, and pollen (Fig. 2G, L). The funiculi of the siliques were also shown to contain GUS activity (Fig. 2M).

The performance of the *AtSCP2* promoter-GUS fusion was also assayed in response to light, darkness, and sucrose in 1–7-d-old seedlings (Fig. 3). The 1-d-old seedlings showed high levels of GUS-activity, indicating high levels of activity of the *AtSCP2* promoter early during germination. There was a decrease in expression from the *AtSCP2* promoter with time, as 7-d-old seedlings showed lower GUS activity compared with 1-d-old and 3-d-old seedlings. Dark-grown seedlings showed a more intense staining, indicating a higher activity of the *AtSCP2* promoter. Interestingly, the GUS activity increased with

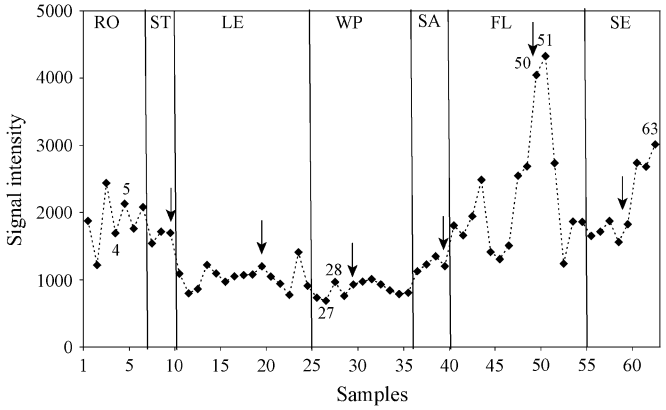

Fig. 1. Expression of *AtSCP2* in *A. thaliana* tissues. The data are collected from the microarray experiment AtGenExpress: Expression Atlas of *A. thaliana* (Schmid *et al*., 2005) obtained from www.weigelworld.org. The investigated tissue samples are from roots (RO) (samples 1–7), stems (ST) (samples 8–10), leaves (LE) (samples 11–25), whole plants (WP) (samples 26–36), shoot apex (SA) (samples 37–40), floral organs (FL) (samples 41–55), and seeds (samples 56–63) of *A. thaliana* Col-0. Samples referred to in the text (4, 5, 27, 28, 50, 51, and 63) are indicated with sample numbers. Samples 10, 20, 30, 40, 50, and 60 are indicated with arrows to simplify for the reader. Plants were grown on soil, unless growth substrate is indicated. (1) Root, 7 d, (2) Root, 17 d, (3) Root, 1×MS agar, 1% sucrose, 15 d, (4) Root, 8 d, 1×MS, (5) Root, 8 d, 1×MS agar, 1% sucrose, (6) Root, 1× MS agar, 21 d, (7) Root, 1×MS agar, 1% sucrose, 21 d, (8) Hypocotyl, 7 d, (9) 1st node, 21+ d, (10) 2nd internode, 21+ d, (11) Cotyledons, 7 d, (12) Leaves no. 1+2, 7 d, (13) Rosette leaf no. 4, 10 d, (14) Rosette leaf no. 2, 17 d, (15) Rosette leaf no. 4, 17 d, (16) Rosette leaf no. 6, 17 d, (17) Rosette leaf no. 8, 17 d, (18) Rosette leaf no. 10, 17 d, (19) Rosette leaf no. 12, 17 d, (20) Petiole leaf no. 7, 17 d, (21) Proximal half leaf no. 7, 17 d, (22) Distal half leaf no. 7, 17 d, (23) Leaf, 1× MS agar, 1% sucrose, 15 d, (24) Senescing leaves, 35 d, (25) Cauline leaves, 21+ d, (26) Seedling, green parts, 7 d, (27) Seedling, green parts, 1× MS agar, 8 d, (28) Seedling, green parts, 1× MS agar, 1% sucrose, 8 d, (29) Seedling, green parts, 1× MS agar, 21 d, (30) Seedling, green parts, 1× MS agar, 1% sucrose, 21 d, (31) Rosette after transition to flowering, but before bolting, 21 d, (32) Rosette after transition to flowering, but before bolting, 22 d, (33) Rosette after transition to flowering, but before bolting 23 d, (34) Vegetative rosette, 7 d, (35) Vegetative rosette, 14 d, (36) Vegetative rosette, 21 d, (37) Shoot apex, vegetative+young leaves, 7 d, (38) Shoot apex, vegetative, 7 d, (39) Shoot apex, transition (before bolting), 14 d, (40) Shoot apex, inflorescence (after bolting), 21 d, (41) Flower, stage 9, (42) Flower, stage 10–11, (43) Flower, stage 12, (44) Flower, stage 15, (45) Flower, 28 d, (46) Pedicel, stage 15, (47) Sepal, stage 12, (48) Sepal, stage 15, (49) Petal, stage 12, (50) Petal, stage 15, (51) Stamen, stage 12, (52) Stamen, stage 15, (53) Pollen, 6 weeks, (54) Carpel, stage 12, (55) Carpel, stage 15, (56) Siliques, with seeds stage 3; mid-globular to early heart embryos globular embryo, (57) Siliques, with seeds stage 4; early to late heart embryos, (58) Siliques, with seeds stage 5; late heart to mid-torpedo embryos triangle embryo, (59) Seeds, stage 6, w/o siliques; mid to late torpedo embryos torpedo embryo, (60) Seeds, stage 7, w/o siliques; late torpedo to early walking-stick embryos walking stick seed, (61) Seeds, stage 8, w/o siliques; walking-stick to early curled cotyledons embryos, (62) Seeds, stage 9, w/o siliques; curled cotyledons to early green cotyledons embryos, (63) Seeds, stage 10, w/o siliques; green cotyledons embryos.

increasing amounts of sucrose when grown under constant illumination as well as in darkness. The microarray data compiled in Fig. 1 also revealed a slight increase in the accumulation of the *AtSCP2* transcript in seedlings in response to sucrose (compare samples 4 and 5, and samples 27 and 28).

Correlated expression patterns of AtSCP2 *to other genes*

To establish a functional context of the expression pattern of *AtSCP2*, it was analysed whether its expression is correlated to that of other genes. To calculate Pearson correlation coefficients (R) from microarray analysis of gene expression, the gene correlator function of Genevestigator (www.genevestigator.ethz.ch) (Zimmermann *et al*., 2004, 2005) and the ExpressionAngler function of the Botany Array Resource in the University of Toronto (bbc.botany.utoronto.ca) (Toufighi *et al*., 2005) were used. Results from such investigations using ExpressionAngler on data from the AtGenExpress experiments are shown in Fig. 4. At the ExpressionAngler, the data are divided into four groups: tissue, hormone, stress, and pathogen for samples collected from various tissues and developmental stages, after hormone treatments, after abiotic stresses or biotic stresses, respectively. The 100 genes from each group giving the highest R to *AtSCP2* were listed. The R cut-off values required for genes to appear on the TOP100-lists were R=0.923 (hormone), R=0.800 (stress), R=0.656 (pathogen), and R=0.686 (tissue). R >0.7 is generally considered a rule-of-thumb threshold for true correlation and used in various analysis (Lee *et al*., 2004; Ren *et al*., 2005). Figure 4 shows the R of the 26 genes that were identified in the lists from at least two of the four groups. Firstly, it can be noted that no gene was found in all the lists, and that only one gene (At4g07390 encoding a PQ-loop repeat family protein) appeared in three of the lists. Of the 25 remaining genes there are three genes (*MFP2*, *PED1*, and *PMDH1*) which encode proteins involved in the β-oxidation cycle (Hayashi *et al*., 1998; Rylott *et al*., 2006; Pracharoenwattana *et al*., 2007). The correlation of expression between *MFP2* and *AtSCP2* is particularly strong, with R=0.82 for tissue samples and R=0.99 for the hormone samples.

Characterization of an AtSCP2 T-DNA *insertion mutant*

To elucidate the biological role of AtSCP2 further, the T-DNA insertion line Sail_1231_F11 was obtained from NASC (Fig. 5A). The Sail_1231_F11 line is referred to as *Atscp2-1*. In *Atscp2-1* the T-DNA insertion is in the second intron of *AtSCP2*. A homozygous insertion line was obtained as confirmed by PCR analysis (Fig. 5B). Transcript analysis using RT-PCR showed that no *AtSCP2* transcript was detected in *Atscp2-1* seedlings (Fig. 5C). Adult plants of *Atscp2-1* were normal in appearance (data not shown). Since the expression analysis revealed the highest levels of the *AtSCP2* transcript in floral tissues and during seed maturation, seed development in *Atscp2-1* was investigated. Thirty-three siliques were removed from wild-type and *Atscp2-1* plants, and the developing seeds were examined under a microscope and counted. For

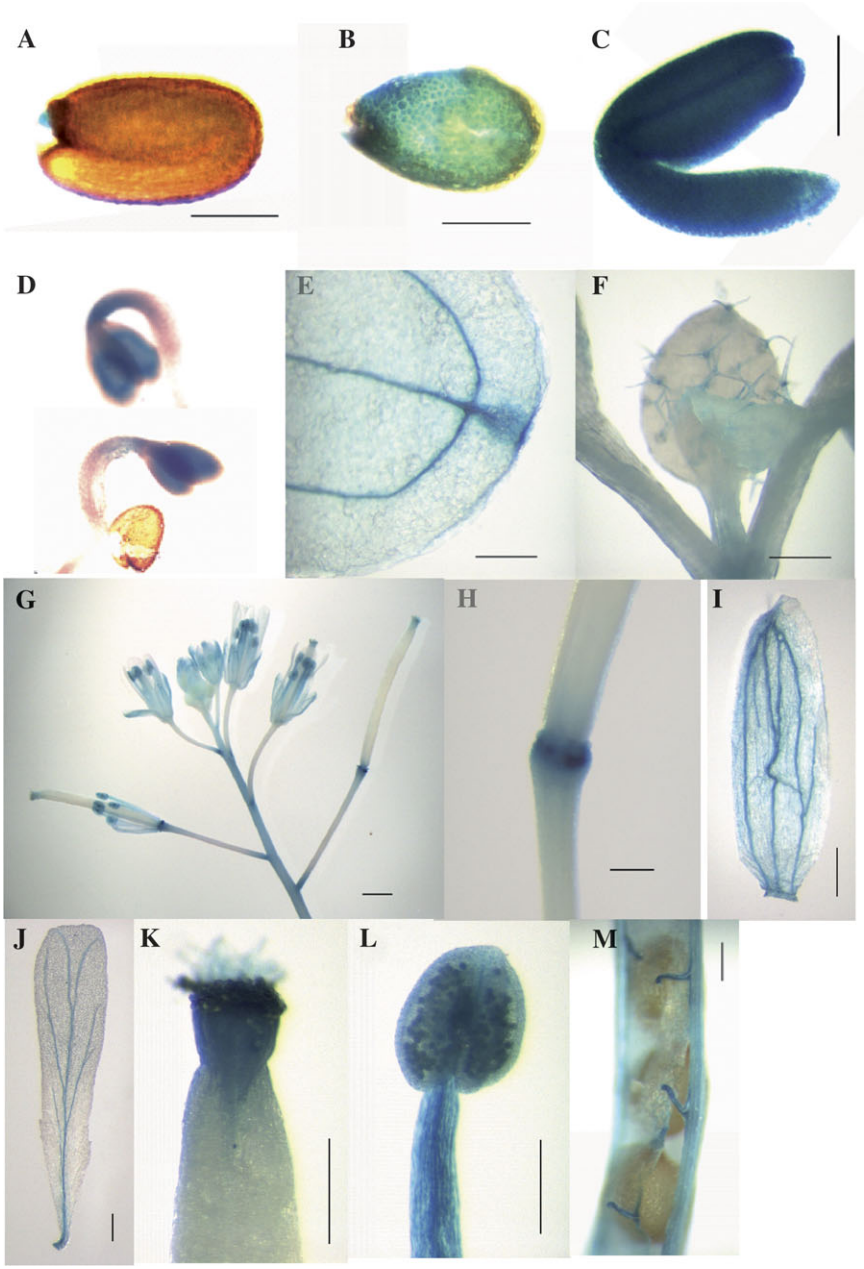

Fig. 2. Localization of GUS protein in transgenic *A. thaliana* plants expressing GUS from the *AtSCP2* promoter. (A) Seed, (B) endosperm, (C) embryo, (D) 2-d-old seedlings, (E) cotyledon hydathode, (F) trichomes, (G) flowers, (H) receptacle, (I) sepal, (J) petal, (K) style, (L) pollen grains, anther and filament, (M) funiculus. GUS activity is visualized by the blue colour. The bar correspond to 200 μm (H, K), 250 μm (A–C, I, J, L), 500 μm (M), 1 mm (F, G) or 2 mm (E).

wild-type plants, the average silique contained 56 green seeds, whereas the average *Atscp2-1* silique contained 49 green seeds. According to the performed *t* test, the seed per silique numbers of *Atscp2-1* were significantly different from wild-type at a *P*-value of 0.000155. When the morphology of the seeds was examined after harvest, it was revealed that seeds from the *Atscp2-1* plants had an imperfect appearance (Fig. 6). Seeds from *Atscp2-1* plants complemented with wild-type *AtSCP-2* from either pJE602 containing a genomic fragment carrying *AtSCP2* including the *AtSCP2* promoter [*Atscp2-1*(*AtSCP2*::*AtSCP2*)] or pJE601 carrying a cDNA copy of *AtSCP2* connected to the CaMV 35S promoter [*Atscp2-1*(35S::*AtSCP2*)] showed wild-type morphology (data not shown).

The germination of *Atscp2-1* seeds was tested by scoring the radicle emergence every 12 h after transferring stratified seeds on 1/2 MS media to a growth chamber. The germination kinetics was significantly slower for *Atscp2-1* seeds compared to wild-type seeds (Fig. 7). 75% of the *Atscp2-1* seeds were germinated after 72 h

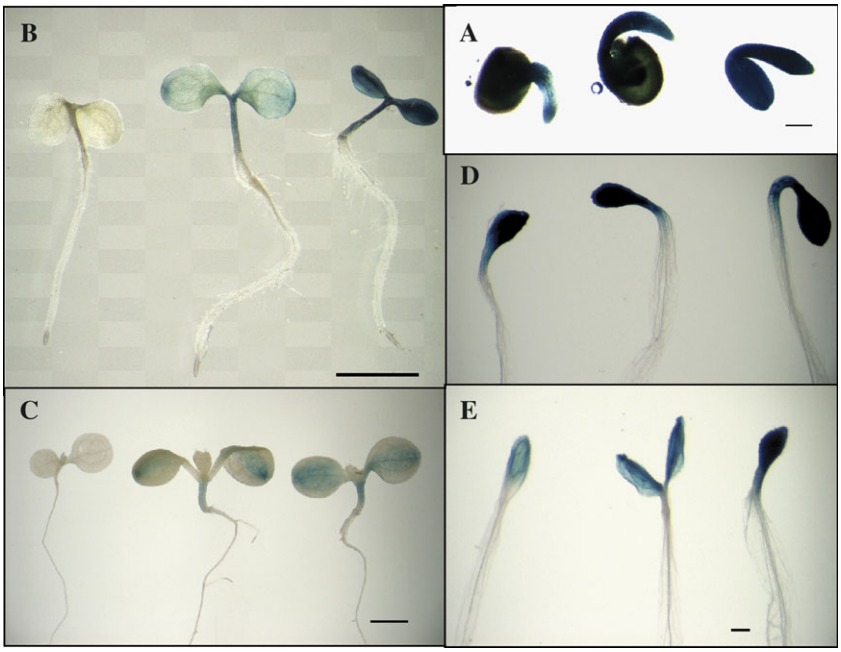

Fig. 3. Sucrose and darkness stimulates expression of GUS from the *AtSCP2* promoter. Seedlings were grown for 1 d (A), 3 d (B, D), or 7 d (C, E) under constant illumination (A–C) or in darkness (D, E) on 1/2 MS agar supplemented with 0% sucrose (leftmost seedling in A–E), 1% sucrose (central seedling in A–E) or 3% sucrose (rightmost seedling in A–E).

incubation showing that the mutant seeds also had a lower germination frequency than the wild-type. Neither the lowered frequency nor the slower kinetics of germination could be rescued by the addition of 1% sucrose to the media. Germination kinetics resembling *A. thaliana* wild-type were obtained when *Atscp2-1* was complemented with wild-type *AtSCP-2* (Fig. 7).

In order to investigate whether the lack of SCP-2 had an effect on seedling establishment, seeds from *Atscp2-1* and wild-type were placed on agar media with or without sucrose and germinated under light or in darkness (Fig. 8). After 3 d on media without sucrose, the *Atscp2-1* seedlings were clearly distinguishable from the wild-type. The insertion line showed smaller cotyledon rosettes and shorter hypocotyls than wild-type and the root elongation was also retarded (Fig. 8A–F). Seven days after sowing the root length was still retarded compared with the wild-type when grown without a carbohydrate supplement (Fig. 8E, F). Also in the dark, root elongation was inhibited on media lacking sucrose as the length of the primary root in *Atscp2-1* was reduced on average to 67% and 48% of the wild-type length when assayed after 3 d and 7 d, respectively. The length of the mutant hypocotyls were slightly reduced in darkness on media lacking sucrose, as they showed a 20% and 14% reduction in length after 3 d and 7 d, respectively. Growth and development of *Atscp2-1* on 1% sucrose closely matched the wild-type control, in light (Fig. 8A–F) as well as in darkness (data not shown).

Effect of 2,4-DB and IBA on germination of AtSCP2 *mutants*

2,4-DB is β-oxidized to 2,4-dichlorophenoxyacetic acid, which inhibits root elongation. Several *A. thaliana* mutants with deficiencies in β-oxidation have been identified in screens for plants that elongated roots on normally inhibitory concentrations of 2,4-DB (Hayashi *et al*., 1998). To investigate whether the AtSCP2 protein may have a role in β-oxidation of auxin precursors and analogues, seeds of *Atscp2-1* were germinated on media containing 0.1 μM and 4 μM 2,4-DB and root elongation was followed. The growth inhibition of root elongation of *Atscp2-1* was indistinguishable from the control wild-type plants on any tested concentration of 2,4-DB indicating that the AtSCP2 is not involved in catabolism of 2,4-DB (data not shown). Several β-oxidation mutants also show resistance to the growth inhibition caused by IBA (Zolman *et al*., 2001; Adham *et al*., 2005). However, *Atscp2-1* also showed wild-type sensitivity to IBA (data not shown).

The binding mode of IBA and 2,4-DB into the homology model of AtSCP2 was studied by the automated docking program GOLD, which gave four docking results for IBA and three results for 2,4-DB. The ligands were positioned quite similarly in all the dockings and only the results with the highest fitness are presented in Fig. 9. Both IBA and 2,4-DB were positioned with their carboxyl groups in one of the cavity openings (near Gln92, Gln110, Ile102, and Leu106). The indole of IBA

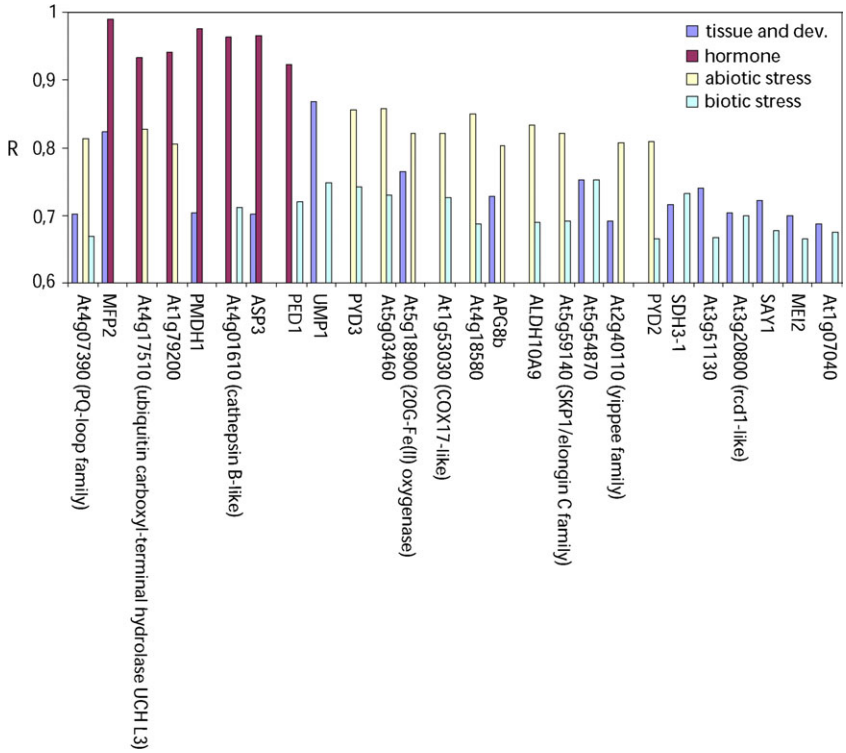

Fig. 4. The expression of AtSCP2 is correlated to the expression of genes involved in β-oxidation. The bar graph shows the Pearson correlation coefficients (*R*) calculated on data from microarray analysis of gene expression. Samples are grouped in tissue and development, hormone treatments, biotic stress, and abiotic stress. Only genes, which were present among the 100 genes with the highest *R* values in at least two sample groups, are included in the graph. *MFP2: MULTIFUNCTIONAL PROTEIN 2; PMDH1: PEROXISOMAL MALATE DEHYDROGENASE 1; ASP3*: *ASPARTATE AMINOTRANSFERASE 3; PED1: PEROXISOME DEFECTIVE 1; UMP1*: *UBIQUITIN-MEDIATED PROTEOLYSIS 1*; *PYD3*: *PYRIMIDINE DEGRADATION STEP 3*; *APG8b*: *AUTOPHAGY-RELATED UBIQUITIN-LIKE MODIFIER 8b*; *ALDH1*: *ALDEHYDE DEHYDROGENASE 1*, *PYD2*: *PYRIMIDINE DEGRADATION STEP 2*; *SDH3-1*: *SUCCINATE DEHYDROGENASE 3–1*; *SAY1*: *STERYL DEACETYLASE 1; MEI2*: *MEIOSIS 2*; *COX17*: Copper chaperone for cytochrome *c* oxidase; *SKP1*: *S-PHASE KINASE-ASSOCIATED PROTEIN*; *rcd1*: *required for cell differentiation 1*.

and the dichlorophenyl group of 2,4-DB were positioned towards the hydrophobic cavity (near Ile37, Phe74, Phe76, Phe81, Met100, and Phe112). The SURFNET plot shows that the AtSCP2 model has a very large tunnel-like cavity. Based on the docking results, the IBA and 2,4-DB molecules take up only a part of the cavity volume and, thus, do not extensively interact with the large hydrophobic cavity, indicating that they are not optimal AtSCP2 ligands (Fig. 9).

Expression profiling of Atscp2-1

To reveal the molecular mechanisms underlying the delayed root elongation of *Atscp2-1* seedlings, expression profiling was performed using the CATMA microarray slides (Allemeersch *et al*., 2005). RNA was isolated from 2-d-old seedlings of wild-type and *Atscp2-1* germinated in the light on media lacking sucrose. The RNA was used as the template for the synthesis of cDNA, which subsequently was labelled with Cy5 and Cy3 and hybridized to the gene-specific tags of 150–500 bp on the microarray slide. The empirical Bayes methods B-statistics (Lönnstedt and Speed, 2002; Smyth *et al*., 2003; Lönnstedt and Britton, 2005) was applied to identify and rank the 100 reporters that, among about 25 000 reporters on the slide, showed the most significant changes in expression pattern in *Atscp2-1*. These 100 reporters corresponded to 94 different genes from the *A. thaliana* genome of which 54 were up-regulated and 40 were down-regulated (including AtSCP2) in *Atscp2-1* (see Supplementary Table S1 at *JXB* online). The expression pattern of 10 genes identified as up- or down-regulated in the microarray analysis was tested with quantitative real-time RT-PCR using gene specific primers. The results confirmed that these genes had a modified expression in *Atscp2-1* (see Supplementary Table S2 at *JXB* online).

Those genes with a significantly altered expression represent a large range of functional categories, such as carbohydrate and amino acid metabolism, transport, and stress response. Interestingly, several genes that previously were shown to have an altered expression in seedlings of *A. thaliana* mutants *icl-2* and *mls-2* with mutations in genes encoding the key enzymes in the glyoxylate cycle, isocitrate lyase (ICL), and malate synthase (MLS) (Cornah *et al*., 2004), also showed an altered expression in *Atscp2-1*

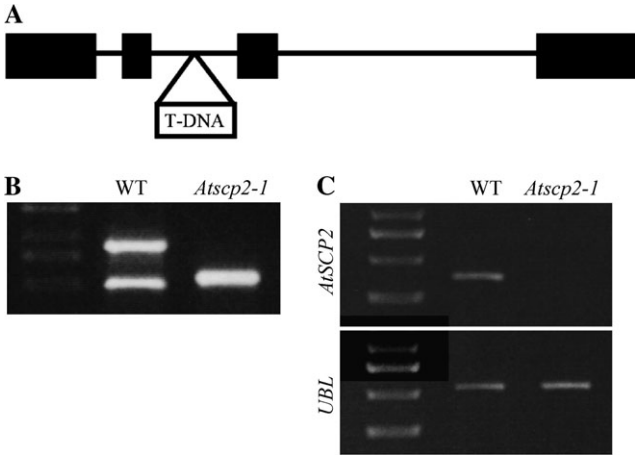

Fig. 5. Characterization of the *Atscp2-1* mutant. In (A) is the genomic structure of the *AtSCP2* loci on chromosome 5 of the *A. thaliana* genome. Exons are indicated as bars. The location of the T-DNA insertion in *Atscp2-1* is shown. (B) PCR analysis of the *AtSCP2* loci in genomic DNA from *A. thaliana* wild-type and *Atscp2-1*. The absence of the *AtSCP2* specific (arrow) PCR product indicates that the *Atscp2-1* line is homozygous for the T-DNA insertion. (C) Analysis of the expression of *AtSCP2* mRNA in wild-type Col-0 and the *Atscp2-1* line. The absence of a PCR product from RT-PCR analysis of *AtSCP2* cDNA shows that *AtSCP2* is not expressed in the *Atscp2-1* line. Information regarding primers is provided in the Materials and methods.

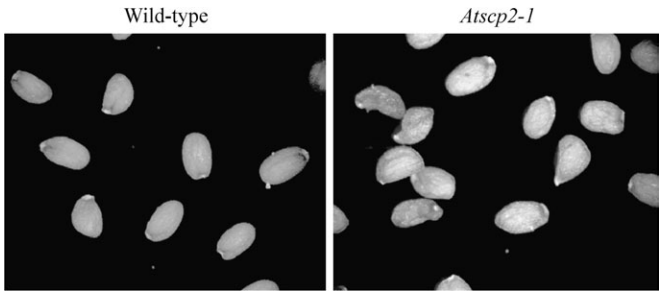

Fig. 6. Seeds from *Atscp2-1* have an aberrant morphology. The picture shows a random sample of seeds from one wild-type plant and one *Atscp2-1* plant.

(Table 1). In fact, of the 20 genes listed showing the most significant overexpression in *icl-2* mutants, six were among the 54 genes that were up-regulated on our Top 100 list. Two out of 12 genes that showed a 2-fold repression in *mls-2*, and 2 out of 10 genes showing a 2-fold overexpression in *mls-2* were also identified in our Top 100 list. Three genes, *ASN1* (At3g47340), At2g05540, and *THA1* (At1g08630), are overexpressed in *Atscp2-1*, *icl-2*, and *mls-2*. ASN1 is a glutamine-dependent asparagine synthase (Lam *et al*., 1994), At2g055490 is a Gly-rich protein, and THA1 is a Thr aldolase, which catalyse the formation of Gly from Thr (Joshi *et al*., 2006).

Metabolome analysis of Atscp2-1

We were interested in identifying metabolites that showed either significantly increased or decreased levels in

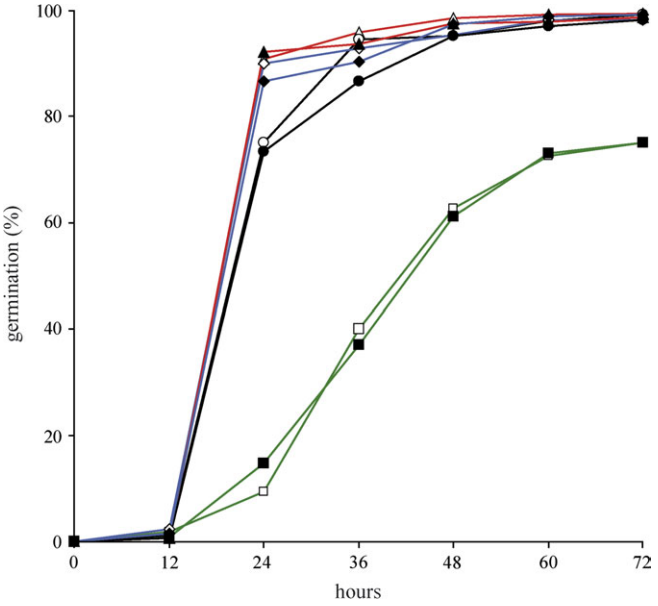

Fig. 7. Seeds from *Atscp2-1* show slower germination kinetics and lower germination frequency. Seeds from wild-type (red lines, triangles), *Atscp2-1* (35S::*AtSCP2*) (black lines, circles), *Atscp2-1* (*AtSCP2*::*AtSCP2*) (blue lines, diamonds), and *Atscp2-1* (green lines, squares) were surface-sterilized and placed on 1/2 MS-media with 1% sucrose (filled symbols) or 0% sucrose (open symbols). Seeds were then stratified for 72 h at 4 °C, and placed in growth cabinet at 22 °C. The time scale measures the time in the growth cabinet. Germination was scored as radicle protrusion. Each time point contains the scoring information from 200–300 seeds.

Atscp2-1. Metabolome analyses were performed on 3-d-old seedlings of *Atscp2-1* and *A. thaliana* wild-type. The samples were extracted, derivatized, and analysed by GC-MS according to Gullberg *et al*. (2004). The GC-MS data were analysed using hierarchical multivariate curve resolution (H-MCR; (Jonsson *et al*., 2005)). The data were centred and scaled to unit variance prior to partial least squares discriminant analysis (PLS-DA) classification of the genotypes. The obtained PLS-DA model (three components; R^2X=0.48; R^2Y=0.99; Q^2Y=0.93) shows a clear separation of the genotypes for the first two components (data not shown). The identification of differences was performed by interpretation of the loadings (as described in Trygg and Wold, 2002) from the PLS-DA model together with the 99% confidence intervals calculated using jack-knifing. In seedlings, 421 variables were detected, 110 of those showed a significant difference between wild-type and *Atscp2-1* according to PLS-DA analysis (one component; R^2X=0.20; R^2Y=0.91; Q^2Y=0.81) and interpretation of first loading vector as described above. The significant metabolites were identified by comparison of retention index and mass spectra with retention index and mass spectra libraries (Schauer *et al*., 2005). The 20 metabolites that showed the most significant difference in accumulation between *Atscp2-1* and wild-type were ranked. Twelve different metabolites

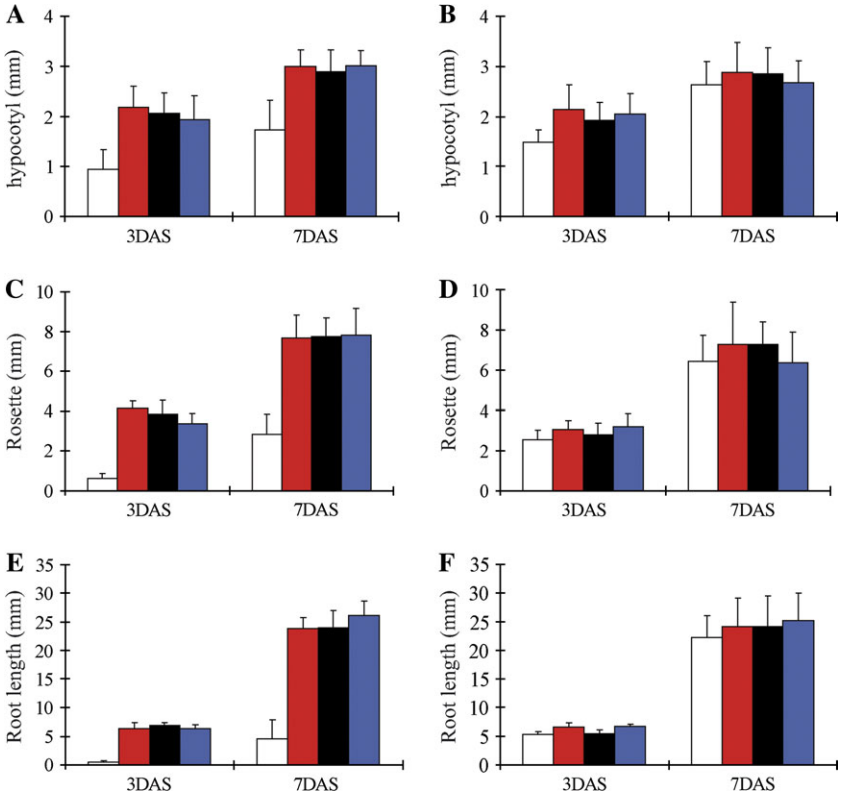

Fig. 8. AtSCP2 is important for root growth during seedling establishment. The hypocotyl length (A, B), size of the rosette (C, D) and root length (E, F) of 3-d-old and 7-d-old seedlings were measured after growing the plants on 1/2 MS without sucrose (A, C, E) or with 1% sucrose (B, D, F) under constant illumination. At least 20 seedlings were measured from each growth condition and time point. White bars: *Atscp2-1*, red bars: wild-type, black bars: *Atscp2-1*(35S::*AtSCP2*), blue bars: *Atscp2-1*(*AtSCP2*::*AtSCP2*). Error bars show standard deviation.

were identified on the ranking list (Table 2). There were higher levels of Gln, pyroglutamic acid (a putative derivatization artefact from glutamate), Asp, β-Ala, fumaric acid, glyceraldehyde, and ribose in wild-type seedlings compared to *Atscp2-1* (Table 2). The *Atscp2-1* seedlings contained enhanced levels of Ser, Gly, Asn, 3-cyanoalanine, and 5-methylthiopentanitrile (tentative identification). Comparison with the previously published metabolome analyses of *icl-2* and *mls-2* seedlings (Cornah *et al*., 2004) revealed several similarities as these mutants were also shown to have lowered amounts of Gln, and that *mls-2* and *Atscp2-1* seedlings both contained increased levels of Ser and Gly. The increased levels of Asn in *Atscp2-1* coincide with increased expression of the asparagine synthase *ASN1*, as shown by the microarray analysis of *Atscp2-1* seedlings. Elevated levels of Gly correlated with increased expression of the Thr aldolase *THA1* in *Atscp2-1*.

Discussion

It has been shown that AtSCP2 is ubiquitously expressed in maturing seeds, young seedlings, and floral tissues, although the transcript is present throughout all developmental stages of *A. thaliana*. The expression of AtSCP2 is correlated to the expression of enzymes of the β-oxidation machinery, such as MFP2, PED1, and PMDH1. The AtSCP2-deficient *Atscp2-1* show altered seed morphology, compromised germination, and require exogenous carbohydrates to avoid delayed seedling establishment. Transcriptome and metabolome analysis of *AtSCP2-1* revealed similarities to the glyoxylate cycle mutants *icl-2* and *mls-2*, such as increased expression of the genes *ASN1* and *THA1*, decreased levels of Gln, and elevated levels of Gly and Ser.

According to current knowledge on β-oxidation and the glyoxylate cycle in *A. thaliana* (reviewed in Baker *et al*., 2006), fatty acids are delivered into the peroxisomes by the peroxisomal ABC-transporter CTS (also referred to as PED3 or PXA1) (Zolman *et al*., 2001; Footitt *et al*., 2002; Hayashi *et al*., 2002). The delivered fatty acids are activated to acyl-CoA esters through the activity of peroxisomal acyl-CoA synthetases such as the long-chain acyl-CoA synthetases LACS6 and LACS7 (Fulda *et al*., 2004). The acyl-CoA esters then go through the repeated cleavage of acetate units from the thiol end through the activities of the β-oxidation enzymes: acyl-CoA oxidases ACX1-6, the multifunctional proteins MFP2 or AIM1,

and the 3-ketoacyl-CoA thiolases (PED1, KAT1 and PKT2) (Hayashi *et al*, 1998, 1999; Richmond and Bleecker, 1999; Germain *et al*., 2001; Adham *et al*., 2005; Rylott *et al*., 2006). To allow for conversion of lipids into sugar via gluconeogenesis, the acetate obtained may be fed into the glyoxylate cycle for the synthesis of succinate, malate, and oxaloacetate. The reactions in the glyoxylate cycle are catalysed by citrate synthase (CSY), aconitase, ICL, MLS, and malate dehydrogenase.

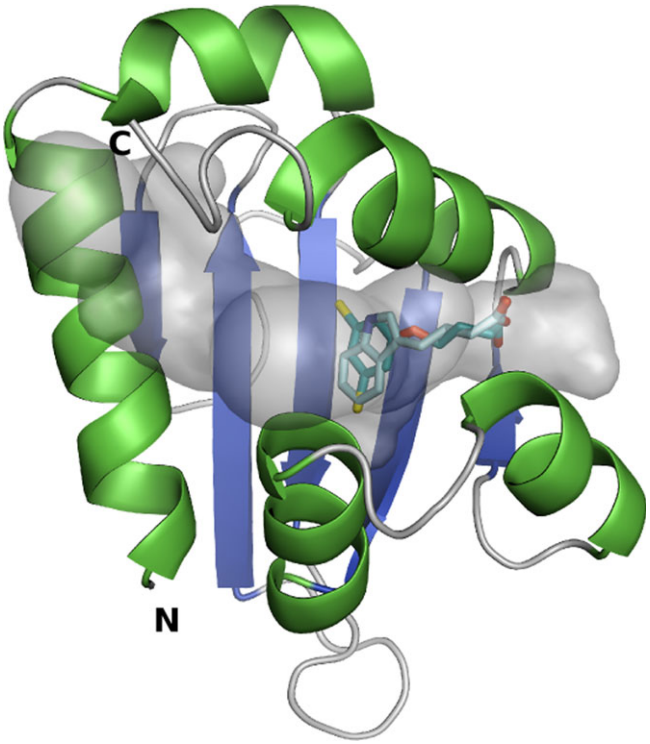

Fig. 9. Docking of IBA and 2,4-DB into the homology model of AtSCP2. The AtSCP2 cavity is shown in transparent grey. IBA and 2,4-DB are shown in light cyan and cyan, respectively. The IBA and 2,4-DB molecules lie near one of the cavity openings and leave a large volume of the binding cavity empty, which suggests that they are not the best possible ligands for AtSCP2.

Seedling establishment of the *Atscp2-1* mutant is not dependent on an exogenous supply of sucrose, but sucrose is required to avoid a delay. Sucrose-dependent seedling establishment has been shown for many *A. thaliana* mutants deficient in proteins with roles in β-oxidation or the glyoxylate cycle, such as the *acx1acx2* mutant deficient in the ACX1 long chain acyl-CoA oxidase and the ACX2 very long chain acyl CoA oxidase (Adham *et al*., 2005), the *aim1* mutant (Richmond and Bleecker, 1999), the *mfp2* mutant (Rylott *et al*., 2006), the *pex6* mutant deficient in a putative peroxisomal ATPase (Zolman and Bartel, 2004), the *pxa1*/*ped3*/*cts* mutant (Zolman *et al*., 2001; Footitt *et al*., 2002; Hayashi *et al*., 2002), the *lacs6lacs7* mutant (Fulda *et al*., 2004), the *ped1*/*kat2* mutant (Hayashi *et al*., 1998; Germain *et al*., 2001), the *csy2csy3* mutant (Pracharoenwattana *et al*., 2005), the *mls-2* mutant (Cornah *et al*., 2004), and the *sdp2* mutant deficient in peroxisomal monohydroascorbate reductase (Eastmond, 2007). The sucrose dependency of these mutants is considered to reflect a lack of gluconeogenesis as a consequence of reduced fatty acid β-oxidation or a blocked glyoxylate cycle.

Many of the above sucrose-dependent mutants with defects in β-oxidation are able to grow in toxic levels of 2,4-DB or IBA. The phenotype of the *Atscp2-1* mutant resembles that of the *mfp2*, *lacs6lacs7*, *acx1acx2*, and *sdp2* mutants, which are sucrose-dependent but still sensitive to 2,4-DB and IBA (Fulda *et al*., 2004; Pinfield-Wells *et al*., 2005; Rylott *et al*., 2006; Eastmond, 2007). The phenotype of the *lacs6lacs7* mutant may be explained by the fact that probably another CoA-synthetase is capable of activating 2,4-DB and IBA to the

Table 1. *Atscp2-1* shows a similar pattern of gene expression as *icl-2* and *mls-1*

The data are from microarray experiments, where the gene expression in *Atscp2-1*, *icl-2*, and *mls-2* seedlings were compared to wild-type seedlings. Only genes ranked to be among the 100 genes showing the most significantly altered expression pattern in *Atscp2-1* were included in the comparison to *icl-2* and *mls-2*. NA, not applicable (see Cornah *et al*., 2004).

Gene	Description[a]	*Atscp2-1*[b]	*icl-2*[bc]	*mls-2*[bc]
THA1 (At1g08630)	Threonine aldolase	+	+	+
At1g21400	2-Oxoisovalerate dehydrogenase	+	+	NA
At2g05540	Gly-rich protein	+	+	+
ASN1 (At3g47340)	Gln-dependent Asn-synthetase	+	+	+
At5g20230	Blue-copper binding protein	+	+	NA
At5g50600	Hydroxysteroid dehydrogenase 1	+	+	NA
At3g14210	Myrosinase-associated protein	–	NA	–
At1g52060	Jasmonate-inducible protein	–	NA	–

[a] Descriptions are according to The Arabidopsis Information Resource (TAIR) at www.arabidopsis.org.
[b] + indicates that the gene is overexpressed in the mutant compared to wild-type; – indicates that the gene is expressed at lower levels in the mutant compared to in wild-type.
[c] Data are from Cornah *et al*. (2004).

Table 2. Compounds showing significantly different levels in 3-d-old seedlings of wild-type and *Atscp2-1*

Compound	Wild-type Relative[a] mean area ±99% confidence interval	*Atscp2-1* Relative[a] mean area ±99% confidence interval
Asp	14 122±3572	8808±2170
β-Ala	798±374	396±65
Fumaric acid	1582±412	887±163
Gln	174 860±37561	89 282±10191
Glyceraldehyde	815±266	323±71
Pyroglutamic acid	312 447±55162	182 199±18855
Ribose	884±265	458±54
Asn	6477±1874	11 380±1560
3-Cyanoalanine	752±100	1171±97
Gly	22 289±3940	50 760±11217
5-Methylthiopentanenitrile[b]	0±0	876±136
Ser	27 879±9060	58 189±5825

[a] Corrected for internal standards and weight.
[b] Tentative identification.

corresponding CoA-thioester before β-oxidation. Moreover, IBA and 2,4-DB sensitivity shows that the deficiency of the two long chain acyl-CoA synthetases does not cause a general block of the β-oxidation cycle in the *lacs6lacs7* mutant. The 2,4-DB sensitivity of *mfp2* mutants is probably due to that the other *A. thaliana* multifunctional protein AIM1 is active on 2,4-DB in a *mfp2* background (Rylott *et al*., 2006). In the case of the *acx1acx2* mutants, the 2,4-DB sensitivity could be due to ACX1 and ACX2 showing specificity for medium to very long chain acyl-CoA species, whereas 2,4-DB is metabolized by ACXs with short-chain specificity as suggested by Pinfield-Wells *et al*. (2005). The 2,4-DB sensitivity shown for *sdp2* was hypothesized to be due to many peroxisomal matrix and membrane proteins remaining functional in the mutant (Eastmond, 2007). The IBA and 2,4-DB sensitivity of the *Atscp2-1* mutant show that AtSCP2 is not required for β-oxidation of those compounds, and that the β-oxidation cycle is not blocked in the mutant. Furthermore, the docking analysis of IBA and 2,4-DB shows that they are not the most favourable ligands for AtSCP2, indicating that AtSCP2 would not be involved in the binding or transfer of the auxin precursors.

The *Atscp2-1* mutant shows a compromised germination, with slower germination kinetics as well as a lower germination frequency. Unlike the post-germinative growth phenotype, the germination phenotype of *Atscp2-1* is not rescued by the addition of exogenous sugar. The slow germination phenotype of *Atscp2-1* resembles the phenotype of the *lac6lac7* double mutant which reached 50% germination in 4.5 d compared to 1.5 d for wild-type (Footitt *et al*., 2006). Sucrose-independent germination phenotypes have also been shown for *acx1acx2*, *ped1*/*kat2*, and *cts* mutants (Pinfield-Wells *et al*., 2005). Seeds from these mutants showed germination frequencies below 30%, indicating a more severe block in germination compared to *Atscp2-1*. Seeds from *ped1*/*kat2* and *cts* mutants contain significant amounts of sucrose (Footitt *et al*., 2002; Pritchard *et al*., 2002) suggesting that the germination phenotypes are not due to a limited supply of soluble sugars. Rather, as suggested recently (Pinfield-Wells *et al*., 2005) the β-oxidation pathway may, during germination, be utilized for the synthesis of a specific signal molecule promoting germination, or to degrade a molecule that inhibits germination. This capacity may then be compromised in *Atscp2-1*, *lac6lac7*, *acx1acx2*, *ped1*/*kat2*, and *cts* mutants leading to an inhibition of germination.

During development and maturation of *A. thaliana* seeds, the total fatty acid levels in the seeds increase, until the later stages of seed maturation when the levels drop to close to 30% relative to the peak levels (Baud *et al*, 2002). Metabolic studies of developing embryos of *Brassica napus* showed that at least 10% of the fatty acids stored as triacylglycerol was lost during the desiccation phase of seed development. Interestingly, metabolic labelling of the embryos revealed that β-oxidation was not associated with net gluconeogenic activity (Chia *et al*., 2005). The function of fatty acid breakdown during seed development remains unclear, nevertheless, the activity during seed maturation may explain the altered morphology of the *Atscp2-1* seeds if AtSCP2 is involved in peroxisomal lipid utilization. We were somewhat surprised to find that sucrose stimulated the expression of *AtSCP2*. Rather, it had been expected that sucrose would repress the expression, as increased levels of sucrose could be signalling a limited need for lipid utilization. Further investigations of the function of AtSCP2 may possibly reveal the significance of this observation.

The *Atscp2-1* seedlings had elevated levels of Asn, Ser, and Gly, and decreased levels of Asp, Glu, and Gln. Changed levels of Gln, Ser, and Gly were previously reported for *icl-2* and *mls-2* seedlings (Cornah *et al*., 2004). Asn accumulates in response to sugar starvation, probably due to an increase in expression of Asn synthase (Lam *et al*., 1994; Azevedo *et al*., 2006), which catalyses the formation of Asn through the transfer of an amide group from Gln to Asp. Our microarray experiments revealed overaccumulation of the *ASN1* transcript in *Atscp2-1* seedlings (see Supplementary Table S1 at *JXB* online) which suggests that the modified levels of Asn, Asp, Gln, and Glu in the *Atscp2-1* mutant are consequences of increased accumulation of Asn synthase. Interestingly, ASN1 had elevated expression levels also in *icl-2* and *mls-2* seedlings (Cornah *et al*., 2004). Why are deficiencies in AtSCP2, ICL, and MLS leading to increased expression of *ASN1*? Possibly, when an exogenous carbon source is lacking, these mutant seedlings are in a condition suggestive of sugar starvation. Sugar starvation triggers *ASN1* expression and leads to increased levels of Asn. *Atscp2-1* also had increased levels of Gly and Ser. This was also seen for the *mls-2* seedlings. In the

case of *mls-2*, Cornah *et al*. (2004) hypothesized that when the glyoxylate cycle is blocked at MLS, glyoxylate feeds into the photorespiratory pathway. The increased activity of the photorespiratory pathway then leads to elevated levels of Gly and Ser. The elevated levels of Gly and Ser in *Atscp2-1* possibly indicate that AtSCP2 also functions in the glyoxylate cycle. This hypothesis may also be supported by the decreased levels of fumarate in *Atscp2-1*. An underperforming glyoxylate cycle in *Atscp2-1* may lead to lowered levels of fumarate, as fumarate is produced in the citric acid cycle from succinate, which is a product of the glyoxylate cycle. The elevated Gly levels may also, at least partially, be due to the demonstrated overexpression of *THA1* in *Atscp2-1*. THA1, which is mainly expressed in seeds and young seedlings, encodes a Thr aldolase functioning in Thr catabolism where it is catalysing the conversion of Thr to Gly (Joshi *et al*., 2006). A *tha1* mutant has a 50% decrease in Gly content (Joshi *et al*., 2006), which indicates that it is not unlikely that the overexpression of *THA1* in *Atscp2-1* would result in elevated Gly levels. It is interesting that the expression of *THA1* was also induced in *mls-2* and *icl-2* seedlings (Cornah *et al*, 2004).Thus, it can not be excluded that the elevated Gly levels in *mls-2* seedlings is, to some extent, related to increased THA1 activity.

We have presented data here showing that the activity of the peroxisomal protein AtSCP2 is important for metabolism in *A. thaliana*. A function in β-oxidation is supported from the co-expression with MFP2, PED1, and PMDH1. The common pattern seen in animals, fungi, and protists with fusions of SCP-2 domains to catalytic domains involved in β-oxidation could also support a direct involvement in β-oxidation for AtSCP2. However, the 2,4-DB-sensitivity shown for *Atscp2-1* may suggest that AtSCP2 is not required for β-oxidation, at least not for all compounds. A function related to the glyoxylate cycle is supported by the similarities between *Atscp2-1* and the glyoxylate cycle mutants *icl-2* and *mls-2*, as revealed by transcriptome and metabolome analyses. Another possibility that cannot be excluded is that the function of AtSCP2 is not directly connected to a specific metabolic pathway. Rather, AtSCP2 could be involved in the transport, solubilization, and presentation of hydrophobic reaction intermediates from several metabolic pathways. Further detailed investigations, including lipid profiling of *Atscp2-1* seedlings, as well as AtSCP2-protein and AtSCP2-ligand interactions may provide us with additional clues to the biological function of AtSCP2.

Supplementary data

Supplementary data are available at *JXB* online.

Table S1. Ranking of genes with significantly altered expression in *Atscp2-1* relative to wild-type.

Table S2. Comparison of results from microarray and quantitative real-time reverse transcriptase PCR (qRT-PCR) analysis of gene expression in wild-type and *Atscp2-1* seedlings.

Acknowledgements

We thank Maria Andersson, Gunilla Swärd, and Gun Rönnqvist for technical assistance, Kristina Blomqvist for comments on the manuscript, and Jens Sundström for tubulin primers and advice on real-time PCR. We thank Anette Hagberg for help with designing and analysing microarray experiments. This work was supported by The Swedish Research Council (JE), Carl Trygger Foundation (JE), China Scholarship Council (BSZ), and the Natural Science Foundation of Zhejiang Province (Y305314) (BSZ).

References

Adamski J, Normand T, Leenders F, Monte D, Begue A, Stehelin D, Jungblut PW, de Launoit Y. 1995. Molecular cloning of a novel widely expressed human 80 kDa 17 β-hydroxysteroid dehydrogenase IV. *Biochemical Journal* **311,** 437–443.

Adham AR, Zolman BK, Millius A, Bartel B. 2005. Mutations in Arabidopsis acyl-CoA oxidase genes reveal distinct and overlapping roles in beta-oxidation. *The Plant Journal* **41,** 859–874.

Allemeersch J, Durinck S, Vanderhaeghen R, *et al.* 2005. Benchmarking the CATMA microarray. A novel tool for Arabidopsis transcriptome analysis. *Plant Physiology* **137,** 588–601.

Azevedo RA, Lancien M, Lea PJ. 2006. The aspartic acid metabolic pathway, an exciting and essential pathway in plants. *Amino Acids* **30,** 143–162.

Baker A, Graham IA, Holdsworth M, Smith SM, Theodoulou FL. 2006. Chewing the fat: β-oxidation in signalling and development. *Trends in Plant Science* **11,** 124–132.

Baud S, Boutin JP, Miquel M, Lepiniec L, Rochat C. 2002. An integrated overview of seed development in *Arabidopsis thaliana* ecotype WS. *Plant Physiology and Biochemistry* **40,** 151–160.

Bloj B, Hughes ME, Wilson DB, Zilversmit DB. 1978. Isolation and amino acid analysis of a nonspecific phospholipid transfer protein from rat liver. *FEBS Letters* **96,** 87–89.

Chia TY, Pike MJ, Rawsthorne S. 2005. Storage oil breakdown during embryo development of *Brassica napus* (L.). *Journal of Experimental Botany* **56,** 1285–1296.

Choinowski T, Hauser H, Piontek K. 2000. Structure of sterol carrier protein 2 at 1.8 Å resolution reveals a hydrophobic tunnel suitable for lipid binding. *Biochemistry* **39,** 1897–1902.

Clough SJ, Bent AF. 1998. Floral dip: a simplified method for *Agrobacterium*-mediated transformation of *Arabidopsis thaliana*. *The Plant Journal* **16,** 735–743.

Cornah JE, Germain V, Ward JL, Beale MH, Smith SM. 2004. Lipid utilization, gluconeogenesis, and seedling growth in Arabidopsis mutants lacking the glyoxylate cycle enzyme malate synthase. *Journal of Biological Chemistry* **279,** 42916–42923.

Curtis MD, Grossniklaus U. 2003. A gateway cloning vector set for high-throughput functional analysis of genes *in planta*. *Plant Physiology* **133,** 462–469.

Dyer DH, Lovell S, Thoden JB, Holden HM, Rayment I, Lan Q. 2003. The structural determination of an insect sterol carrier protein-2 with a ligand-bound C16 fatty acid at 1.35A resolution. *Journal of Biological Chemistry* **278,** 39085–39091.

Eastmond PJ. 2007. MONODEHYROASCORBATE REDUCTASE4 is required for seed storage oil hydrolysis and postgerminative growth in *Arabidopsis*. *The Plant Cell* **19,** 1376–1387.

Edqvist J, Blomqvist K. 2006. Fusion and fission, the evolution of sterol carrier protein-2. *Journal of Molecular Evolution* **62,** 292–306.

Edqvist J, Rönnberg E, Rosenquist S, Blomqvist K, Viitanen L, Salminen TA, Nylund M, Tuuf J, Mattjus P. 2004. Plants express a lipid transfer protein with high similarity to mammalian sterol carrier protein-2. *Journal of Biological Chemistry* **279,** 53544–53553.

Eklund DM, Edqvist J. 2003. Localization of non-specific lipid transfer proteins correlate with programmed cell death responses during endosperm degradation in *Euphorbia lagascae* seedlings. *Plant Physiology* **132,** 1249–1259.

Footitt S, Slocombe SP, Larner V, Kurup S, Wu Y, Larson T, Graham I, Baker A, Holdsworth M. 2002. Control of germination and lipid mobilization by COMATOSE, the Arabidopsis homologue of human ALDP. *EMBO Journal* **21,** 2912–2922.

Footitt S, Marquez J, Schmuths H, Baker A, Theodoulou FL, Holdsworth M. 2006. Analysis of the role of COMATOSE and peroxisomal β-oxidation in the determination of germination potential in *Arabidopsis*. *Journal of Experimental Botany* **57,** 2805–2814.

Fulda M, Schnurr J, Abbadi A, Heinz E, Browse J. 2004. Peroxisomal acyl-CoA synthetase activity is essential for seedling development in *Arabidopsis thaliana*. *The Plant Cell* **16,** 394–405.

Germain V, Rylott EL, Larson TR, Sherson SM, Bechtold N, Carde JP, Bryce JH, Graham IA, Smith SM. 2001. Requirement for 3-ketoacyl-CoA thiolase-2 in peroxisome development, fatty acid β-oxidation and breakdown of triacylglycerol in lipid bodies of *Arabidopsis* seedlings. *The Plant Journal* **28,** 1–12.

Gullberg J, Jonsson P, Nordström A, Sjöström M, Moritz T. 2004. A strategy for identifying differences in large series of metabolomic samples analysed by GC/MS. *Analytical Chemistry* **76,** 1738–1745.

Haapalainen AM, van Aalten DM, Merilainen G, Jalonen JE, Pirila P, Wierenga RK, Hiltunen JK, Glumoff T. 2001. Crystal structure of the liganded SCP-2-like domain of human peroxisomal multifunctional enzyme type 2 at 1.75 Å resolution. *Journal of Molecular Biology* **313,** 1127–1138.

Hayashi H, De Bellis L, Ciurli A, Kondo M, Hayashi M, Nishimura M. 1999. A novel acyl-CoA oxidase that can oxidize short-chain acyl-CoA in plant peroxisomes. *Journal of Biological Chemistry* **274,** 12715–12721.

Hayashi M, Nito K, Takei-Hoshi R, Yagi M, Kondo M, Suenaga A, Yamaya T, Nishimura M. 2002. Ped3p is a peroxisomal ATP-binding cassette transporter that might supply substrates for fatty acid β-oxidation. *Plant and Cell Physiology* **43,** 1–11.

Hayashi M, Toriyama K, Kondo M, Nishimura M. 1998. 2,4-Dichlorophenoxybutyric acid-resistant mutants of Arabidopsis have defects in glyoxysomal fatty acid β-oxidation. *The Plant Cell* **10,** 183–195.

Jefferson RA, Kavanagh TA, Bevan MW. 1987. GUS fusions: β-glucuronidase as a sensitive and versatile gene fusion marker in higher plants. *EMBO Journal* **6,** 3901–3907.

Jones G, Willett P, Glen RC. 1995. Molecular recognition of receptor sites using a genetic algorithm with a description of desolvation. *Journal of Molecular Biology* **245,** 43–53.

Jones G, Willett P, Glen RC, Leach AR, Taylor R. 1997. Development and validation of a genetic algorithm for flexible docking. *Journal of Molecular Biology* **267,** 727–748.

Joshi V, Laubengayer KM, Schauer N, Fernie AR, Jander G. 2006. Two Arabidopsis threonine aldolases are nonredundant and compete with threonine deaminase for a common substrate pool. *The Plant Cell* **18,** 3564–3575.

Jonsson P, Johansson A, Gullberg J, Trygg J, Jiye A, Grung B, Marklund S, Sjöström M, Antti H, Moritz T. 2005. High through-put data analysis for detecting and identifying differences between samples in GC/MS-based metabolomic analyses. *Analytical Chemistry* **77,** 5635–5642.

Kiema TR, Taskinen JP, Pirila PL, Koivuranta KT, Wierenga RK, Hiltunen JK. 2002. Organization of the multifunctional enzyme type 1: interaction between N- and C-terminal domains is required for the hydratase-1/isomerase activity. *Biochemical Journal* **367,** 433–441.

Lam HM, Peng SS, Coruzzi GM. 1994. Metabolic regulation of the gene encoding glutamine-dependent asparagine synthetase in *Arabidopsis thaliana*. *Plant Physiology* **106,** 1347–1357.

Laskowski RA. 1995. SURFNET: a program for visualizing molecular surfaces, cavities, and intermolecular interactions. *Journal of Molecular Graphics* **13,** 323–330.

Lee HK, Hsu AK, Sajdak J, Qin J, Pavlidis P. 2004. Co-expression analysis of human genes across many micro array data sets. *Genome Research* **14,** 1085–1094.

Leenders F, Dolez V, Begue A, Moller G, Gloeckner JC, de Launoit Y, Adamski J. 1998. Structure of the gene for the human 17β-hydroxysteroid dehydrogenase type IV. *Mammalian Genome* **9,** 1036–1041.

Lehtonen JV, Still DJ, Rantanen VV, *et al.* 2004. BODIL: a molecular modelling environment for structure-function analysis and drug design. *Journal of Computer-Aided Molecular Design* **18,** 401–419.

Livak KJ, Schmittgen TD. 2001. Analysis of relative gene expression data using real-time quantitative PCR and the $2^{-\overline{\Delta\Delta CT}}$ method. *Methods* **25,** 402–408.

Lönnstedt I, Britton T. 2005. Hierarchical Bayes models for cDNA microarray gene expression. *Biostatistics* **6,** 279–291.

Lönnstedt I, Speed TP. 2002. Replicated microarray data. *Statistica Sinica* **12,** 31–46.

Ohba T, Holt JA, Billheimer JT, Strauss 3rd JF. 1995. Human sterol carrier protein x/sterol carrier protein 2 gene has two promoters. *Biochemistry* **34,** 10660–10668.

Ohba T, Rennert H, Pfeifer SM, He Z, Yamamoto R, Holt JA, Billheimer JT, Strauss 3rd JF. 1994. The structure of the human sterol carrier protein X/sterol carrier protein 2 gene (SCP2). *Genomics* **24,** 370–374.

Pinfield-Wells H, Rylott EL, Gilday AD, Graham S, Job K, Larson TR, Graham IA. 2005. Sucrose rescues seedling establishment but not germination of Arabidopsis mutants disrupted in peroxisomal fatty acid catabolism. *The Plant Journal* **43,** 861–872.

Pracharoenwattana I, Cornah JE, Smith SM. 2005. Arabidopsis peroxisomal citrate synthase is required for fatty acid respiration and seed germination. *The Plant Cell* **17,** 2037–2048.

Pracharoenwattana I, Cornah JE, Smith SM. 2007. Arabidopsis peroxisomal malate dehydrogenase functions in β-oxidation but not in the glyoxylate cycle. *The Plant Journal* **50,** 381–390.

Pritchard SL, Charlton WL, Baker A, Graham IA. 2002. Germination and storage reserve mobilization are regulated independently in Arabidopsis. *The Plant Journal* **31,** 639–647.

Ren XY, Fiers MW, Stiekema WJ, Nap JP. 2005. Local coexpression domains of two to four genes in the genome of Arabidopsis. *Plant Physiology* **138,** 923–934.

Richmond TA, Bleecker AB. 1999. A defect in β-oxidation causes abnormal inflorescence development in Arabidopsis. *The Plant Cell* **11,** 1911–1924.

Ritter MC, Dempsey ME. 1971. Specificity and role in cholesterol biosynthesis of a squalene and sterol carrier protein. *Journal of Biological Chemistry* **246,** 1536–1539.

Rylott EL, Eastmond PJ, Gilday AD, Slocombe SP, Larson TR, Baker A, Graham IA. 2006. The *Arabidopsis thaliana*

multifunctional protein gene (MFP2) of peroxisomal β-oxidation is essential for seedling establishment. *The Plant Journal* **45,** 930–941.

Schauer N, Steinhauser D, Strelkov S, *et al.* 2005. GC-MS libraries for the rapid identification of metabolites in complex biological samples. *FEBS Letters* **579,** 1332–1337.

Schmid M, Davison TS, Henz SR, Pape UJ, Demar M, Vingron M, Scholkopf B, Weigel D, Lohmann JU. 2005. A gene expression map of *Arabidopsis thaliana* development. *Nature Genetics* **37,** 501–506.

Seedorf U, Ellinghaus P, Nofer JR. 2000. Sterol carrier protein-2. *Biochimica et Biophysica Acta* **1486,** 45–54.

Seedorf U, Raabe M, Ellinghaus P, *et al.* 1998. Defective peroxisomal catabolism of branched fatty acyl coenzyme A in mice lacking the sterol carrier protein-2/sterol carrier protein-X gene function. *Genes and Development* **12,** 1189–1201.

Smyth GK, Yang YH, Speed T. 2003. Statistical issues in cDNA microarray data analysis. *Methods in Molecular Biology* **224,** 111–136.

Toufighi K, Brady SM, Austin R, Ly E, Provart NJ. 2005. The Botany Array Resource: e-Northerns, Expression Angling, and promoter analyses. *The Plant Journal* **43,** 153–163.

Trygg J, Wold S. 2002. Orthogonal projections to latent structures (O-PLS). *Journal of Chemometrics* **16,** 119–128.

Viitanen L, Nylund M, Eklund DM, Alm C, Eriksson AK, Tuuf J, Salminen TA, Mattjus P, Edqvist J. 2006. Characterization of SCP-2 from *Euphorbia lagascae* reveals that a single Leu/Met exchange enhances sterol transfer activity. *FEBS Journal* **273,** 5641–5655.

Wanders RJ. 2004. Peroxisomes, lipid metabolism, and peroxisomal disorders. *Molecular Genetics and Metabolism* **83,** 16–27.

Wouters FS, Bastiaens PIH, Wirtz KWA, Jovin TM. 1998. FRET microscopy demonstrates molecular association of non-specific lipid transfer protein (nsL-TP) with fatty acid oxidation enzymes in peroxisomes. *EMBO Journal* **17,** 7179–7189.

Zimmermann P, Hennig L, Gruissem W. 2005. Gene-expression analysis and network discovery using Genevestigator. *Trends in Plant Science* **10,** 407–409.

Zimmermann P, Hirsch-Hoffmann M, Hennig L, Gruissem W. 2004. GENEVESTIGATOR. Arabidopsis microarray database and analysis toolbox. *Plant Physiology* **136,** 2621–2632.

Zolman BK, Bartel B. 2004. An Arabidopsis indole-3-butyric acid-response mutant defective in PEROXIN6, an apparent ATPase implicated in peroxisomal function. *Proceedings of the National Academy of Sciences, USA* **101,** 1786–1791.

Zolman BK, Silva ID, Bartel B. 2001. The Arabidopsis *pxa1* mutant is defective in an ATP-binding cassette transporter-like protein required for peroxisomal fatty acid beta-oxidation. *Plant Physiology* **127,** 1266–1278.